Supporting Information

Nonhalogen Dry Etching of Metal Carbide TiAlC by Low-Pressure N_2/H_2 Plasma at Room Temperature

Thi-Thuy-Nga Nguyen[1,*], Kazunori Shinoda[2], Shih-Nan Hsiao[1], Kenji Maeda[2], Kenetsu Yokogawa[2], Masaru Izawa[2], Kenji Ishikawa[1], and Masaru Hori[1]

[1]Nagoya University, Nagoya 464-8601, Japan

[2]Hitachi High-Tech Corp., Tokyo 105-6409, Japan

[*)] nguyen.thi.thuy.nga.w9@f.mail.nagoya-u.ac.jp (ORCID 0000-0002-2170-2488)

Key words: metal carbide, TiAlC, metal compound etching, nonhalogen dry etching, N_2/H_2 plasma, plasma-surface reaction

Table S1. The best-fit parameters of TiAlC layer obtained by Gen-Osc model.

	E_∞ (eV)		
	2.218		
Drude (RT)	Resistivity (Ω.cm)[4]	Scattering time (fs)[4]	
	2.2902e-06	1000	
	Amplitude (eV)	Broadening (eV)	Energy (eV)
Lorentz 1	4.192038	2.2739	2.425
Lorentz 2	4.098684	1.3546	1.135
Lorentz 3	4.783837	5.1058	5.282

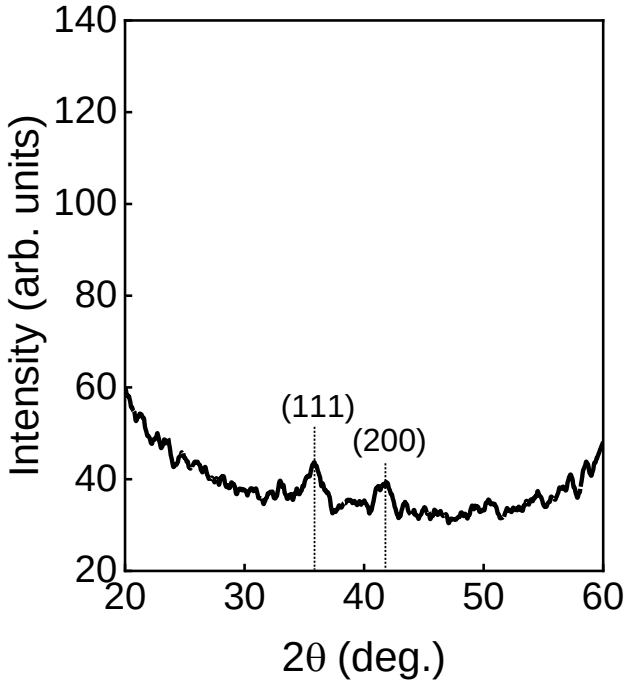

Figure S1. XRD pattern of 35nm-TiAlC film grown on Si wafer by RF ion plating.

Figure S1 shows the XRD pattern of the pristine TiAlC sample. The broaden peaks (111) and (200) at around 35.8^{o} and 41.8^{o} are identified as TiAlC phase, this result is comparable with the study of J. Moon et al.[1] in using plasma-enhanced atomic layer deposition via titanium chloride ($TiCl_4$) and trimethylaluminum (TMA) to grow polycrystalline Al-doped TiC. A quantitative phase analysis in the Ti-Al-C ternary system by X-ray diffraction was done by Wang et al., in which the diffraction peaks at 35.9^{o}, 41.7 ^{o}, and 60.5 ^{o} are assigned for TiC phase.[2] A similar result can be found from the work of Zhang et al.[3] in synthesis of TiAlC by using plasma spraying from Ti/Al/graphite agglomerates and post annealing, the TiC diffraction peaks (36.8◦, 42.6^{o} and 62.1^{o}) are almost close to the TiAlC peaks in this study, in which the (Ti,Al)C_x could be a solid solution of Al in TiC or Al-doped TiC_x. This indicates that the pristine TiAlC sample was used in our study has polycrystal structure that was formed during RF reactive ion plating process. Because the deposition process was controlled at low substrate temperature (less than 100 ^{o}C without any additional heater), C vacancies may exist the pristine polycrystal TiAlC sample.

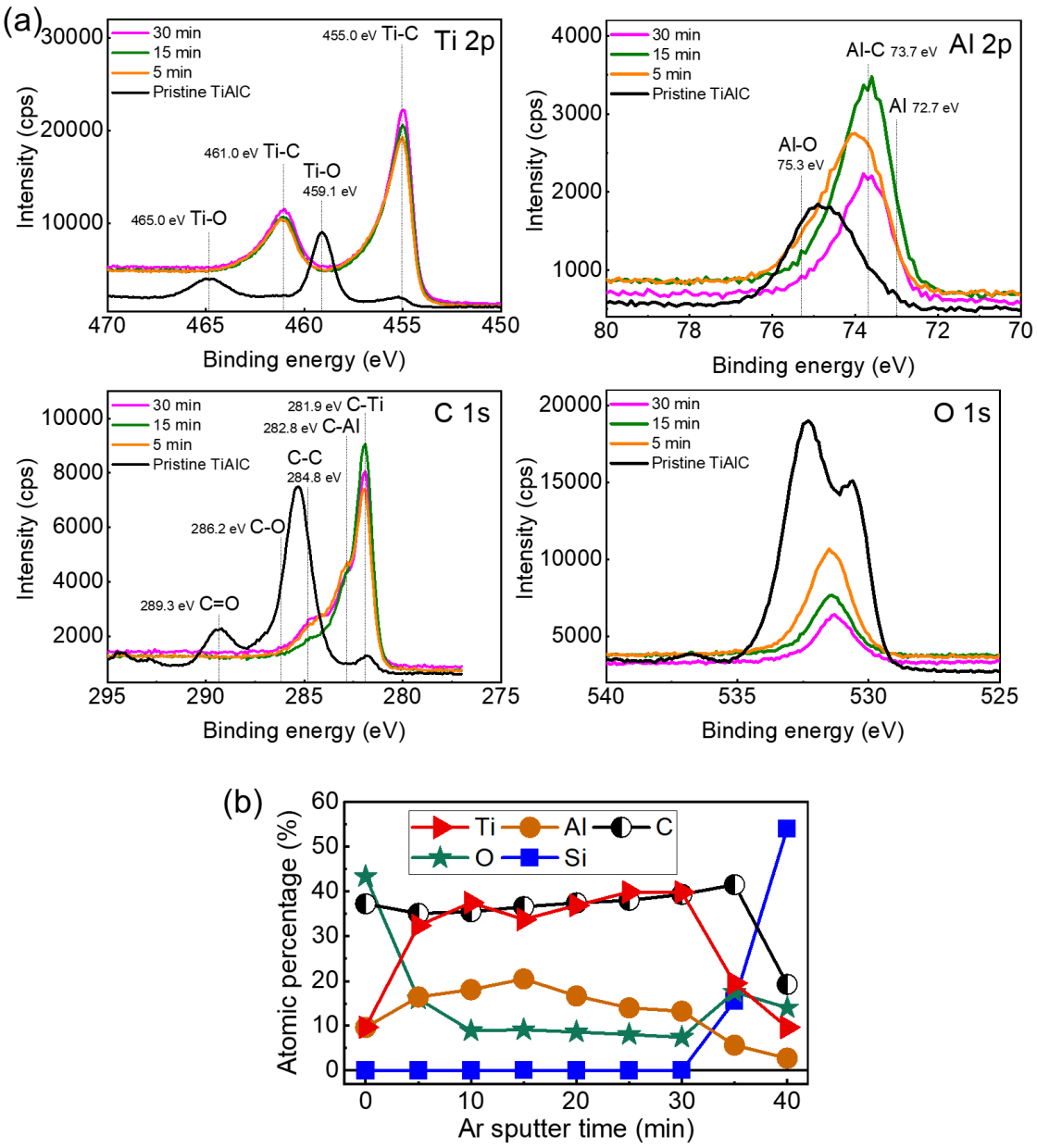

Figure S2. (a) *In situ* XPS spectra of TiAlC before and after Ar sputter in the same XPS chamber. Beam voltage: 5 kV, ion current: 1 μA, sputter area: 4 mm × 4 mm. (b) Dependence of atomic percentage in TiAlC films evaluated by XPS on Ar sputter time.

Figure S2a shows that the Ti $2p_{3/2}$ binding energies are 455.0 eV for Ti-C bond and 461.0 eV for Ti-O bond, respectively. In the C 1s spectrum, the C-Ti, C-Al, C-C, C-O, and C=O bonds are respectively located at 281.9 eV, 282.8 eV, 284.8 eV, 286.2 eV and 289.3 eV. In the Al 2p spectrum, there is a chemical shift of the Al 2p peak from 72.7 eV of pure Al to 73.7 eV in the (Ti,Al)C_x film, and the Al-O bond is located at 75.3 eV. If this shift is in the opposite direction, it is supposed to the $Ti_{n+1}AlC_n$ (MAX phases) which has the Al-C peak

located at a lower binding energy than pure Al.[4] There is no Ti-Al bond existing in the TiAlC film. After removing the native oxide (Al–O, Ti–O, C-O, C=O) around 43.4% oxygen at% from the surface, the at% ratio of Ti:Al:C:O is around 38:18:35:9 (approximately 4:2:4:1) (Figure S2b). Around 9% of oxygen exists inside the TiAlC film. The Al at% is 18%, that is higher than the maximum solubility (1% for at%) of Al in TiC,[5,6] suggesting that the pristine TiAlC sample is a metastable solid solution of Al into the cubic carbide structure or Al-rich precipitations in the cubic TiC film.

Table S2. The atomic radii and atomic weights of the elements used in this study. Data was taken from references. [7,8]

Element	H	C	N	O	Al	Ti
Atomic number	1	6	7	8	13	22
Atomic radius (A^o)	1.54	1.90	1.79	1.71	2.39	2.57
Standard atomic weight	[1.0078, 1.0081]	[12.0096, 12.0116]	[14.0064, 14.0072]	[15.9990, 15.9998]	26.9815	47.8670

Table S3. Film thickness change of TiAlC before and after exposing to N_2/H_2 plasmas at 4 Pa. The data was subtracted from *in situ* ellipsometry measurement, minimizing the re-oxidation of TiAlC surface after the process.

H_2%	Pristine	After N_2/H_2 plasma exposure (4 Pa)		
	Thickness TiAlC (nm)	Thickness TiAlC (nm)	Etch time (min)	Etch rate TiAlC (nm/min)
0.00 (N_2 plasma)	39.79	39.63	10	0.02
33.33	38.68	20.44	10	1.82
50.00	39.96	21.50	10	1.85
66.67	38.43	20.38	10	1.81
100 (H_2 plasma)	39.87	45.97	10	-0.61 (<0, no etching)

Table S4. Details of peak binding energy (BE) and full width at half maximum (FWHM) of TiAlC film before and after exposure to N_2/H_2 plasma.

Element	Chemical bond	Doublet	Pristine TiAlC		After N_2/H_2 plasma	
			Peak BE (eV)	FWHM (eV)	Peak BE (eV)	FWHM (eV)
Ti 2p	Ti-C	$2p_{3/2}$	455.45	0.90	455.44	0.89
		$2p_{1/2}$	461.47	1.09	461.29	1.03
	N-Ti-C	$2p_{3/2}$			456.25	0.90
		$2p_{1/2}$			462.10	1.16
	O-Ti-C	$2p_{3/2}$	456.45	0.90		
		$2p_{1/2}$	462.63	1.11		
	Ti-N	$2p_{3/2}$			457.27	1.25
		$2p_{1/2}$			463.02	1.25
	O-Ti-N	$2p_{3/2}$			458.28	1.30
		$2p_{1/2}$			464.04	1.30
	Ti-O	$2p_{3/2}$	459.44	1.34	459.22	1.39
		$2p_{1/2}$	465.14	2.35	464.74	2.39
Al 2p	Al-Al		73.22	0.80	72.92	0.79
	Al-C		73.98	0.90	73.55	0.90
	Al-N				74.19	1.20
	Al-O		74.80	1.50	75.04	1.49
C 1s	C-Ti		281.84	0.75	281.91	0.72
	C-Al		282.84	0.90	282.68	0.90
	C-C		284.80	1.30	284.80	1.30
	C-N				285.34	1.31
	C-O		285.80	1.29	286.72	1.51
	C=O		287.26	1.50		
	O-C=O		289.60	1.50	288.64	1.50
N 1s	N-Ti(Al)-O				396.42	0.81
	N-Ti(Al)				397.07	1.20
	N-C				398.41	1.51
	N-H				400.07	1.44

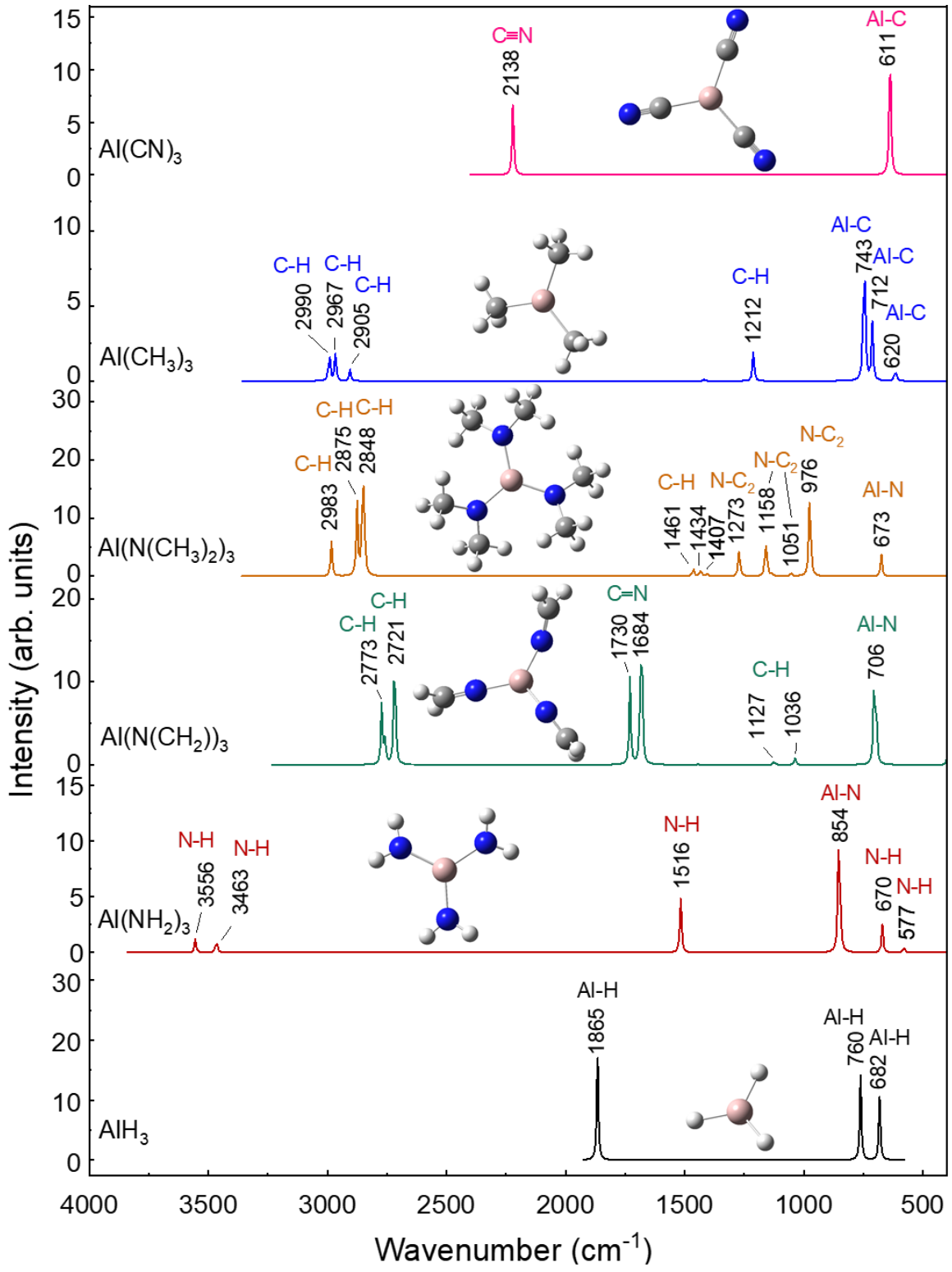

Figure S3. The DFT calculated IR spectra of Al-based organometallic molecules. The insets image are their molecular structures.

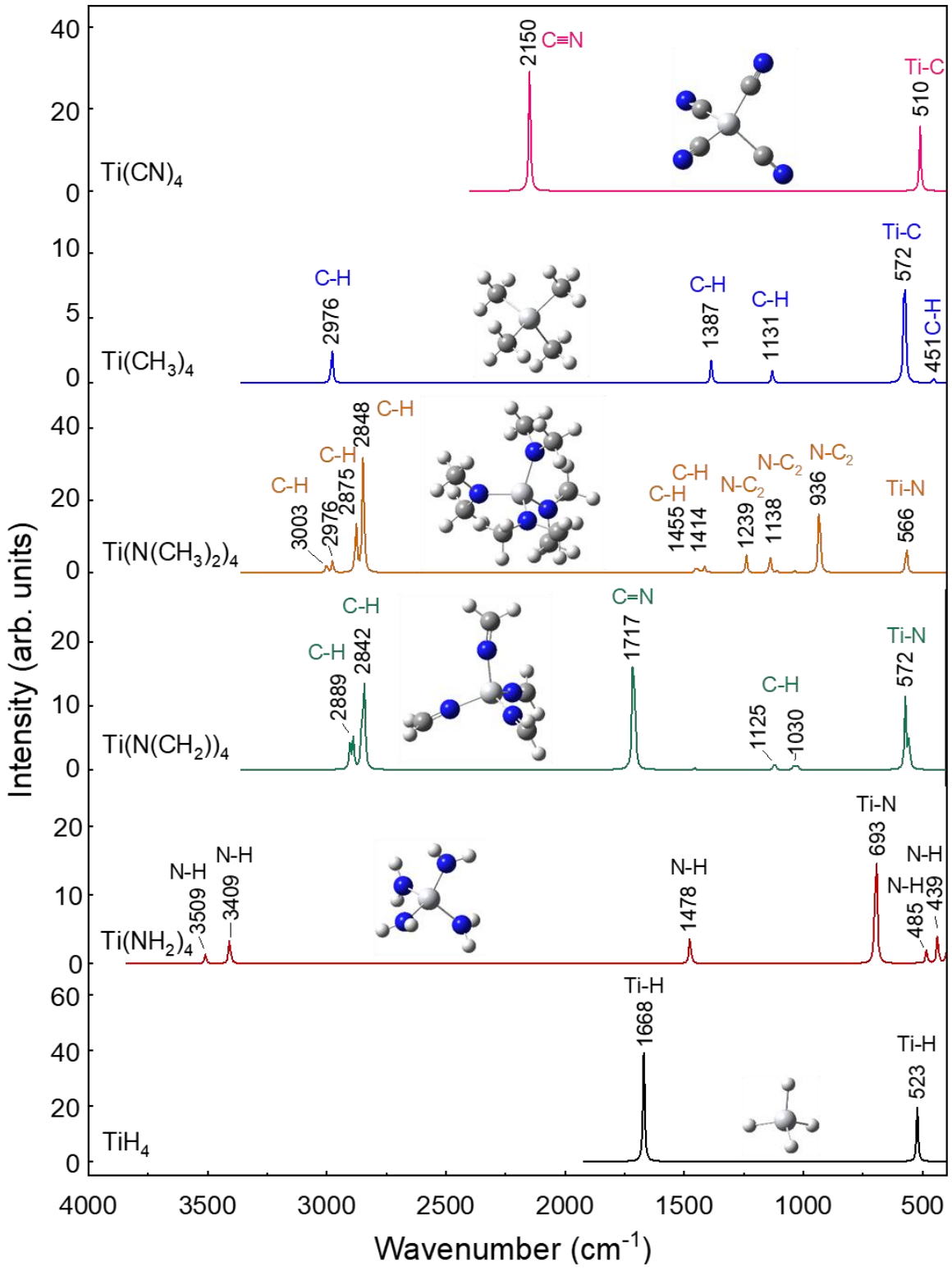

Figure S4. The DFT calculated IR spectra of Ti-based organometallic molecules. The insets image are their molecular structures.

Table S5. Boiling points of potential volatile products (organometallic compounds) formed by the reaction between N_2/H_2 plasma and TiAlC surface.

Organometallic compounds	Abbreviation	Molecular structure	Boiling point (^oC)	Reference
Trimethylaluminum	TMA	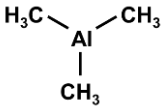	125-126	9,10
Tris(dimethylamido)aluminum (III), dimer	TDMAA dimer	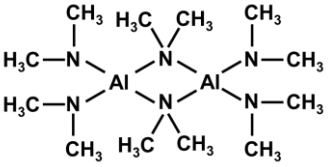	90 (Bubble point)	11
Tetrakis(dimethylamido)titanium (IV)	TDMAT	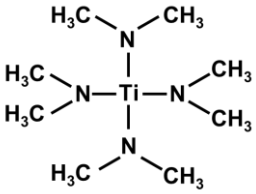	50	12

Table S6. Bond length and bond dissociation energy of metal-metal (M-M) and metal compounds (M-X) such as metal oxides, metal hydrides, metal carbides, metal nitrides used in this study. The values can vary, depending on factors such as composition, crystal structure, synthesis method, measurement method, or calculation method. Data was taken from references. [13-22]

M-M M-X	Bond length (A^o)	Bond energy (kJ/mol)	M-M M-X	Bond length (A^o)	Bond energy (kJ/mol)
Al-Al	2.61-2.86 [14]	186 [13]	Ti-Ti	2.96 [15]	141 [13]
Al-H	1.68-1.78 [14]	285 [13]	Ti-H	1.70 [16,17]	159 [13]
Al-C	3.88 [18]	255 [13]	Ti-C	2.08-2.20 [15,18,19]	435 [13]
Al-N	3.83 [18]	297 [13]	Ti-N	2.09 [18]	464 [13]
Al-O	1.70-1.90 [20]	512 [13]	Ti-O	2.12-2.14 [19]	662 [13]
Al-Ti	2.82-2.91 [15,18,19]	263.4 [21]	N-H	1.01 [22]	314 [13]
C-C	3.14 [15]	607 [13]	C-N	1.47-1.49 [22]	770 [13]

References

(1) Moon, J.; Ahn, H. J.; Seo, Y.; Lee, T. I.; Kim, C. K.; Rho, I. C.; Kim, C. H.; Hwang, W. S.; Cho, B. J. The Work Function Behavior of Aluminum-Doped Titanium Carbide Grown by Atomic Layer Deposition. *IEEE Trans Electron Devices* **2016**, *63* (4), 1423–1427. https://doi.org/10.1109/TED.2016.2527688.

(2) Wang, C.-A.; Zhou, A.; Qi, L.; Huang, Y. Quantitative Phase Analysis in the Ti–Al–C Ternary System by X-Ray Diffraction. *Powder Diffr* **2005**, *20* (3), 218–223. https://doi.org/10.1154/1.1951687.

(3) Zhang, F.; Chen, J.; Yan, S.; Yu, G.; Ma, H.; He, J.; Yin, F. Microstructure and Reaction Mechanism of Ti-Al-C Based MAX Phase Coatings Synthesized by Plasma Spraying and Post Annealing. *Surf Coat Technol* **2022**, *441*. https://doi.org/10.1016/j.surfcoat.2022.128584.

(4) Barsoum, M. W.; Crossley, A.; Myhra, S. Crystal-Chemistry from XPS Analysis of Carbide-Derived Mn+1AXn (N=1) Nano-Laminate Compounds. *Journal of Physics and Chemistry of Solids* **2002**, *63* (11), 2063–2068.

(5) *Handbook of Ternary Alloy Phase Diagrams*; Villars, P., Prince, A., Okamoto, H., Eds.; ASM International, 1995; Vol. 4.

(6) Wilhelmsson, O.; Palmquist, J. P.; Nyberg, T.; Jansson, U. Deposition of Ti2AlC and Ti3AlC2 Epitaxial Films by Magnetron Sputtering. *Appl Phys Lett* **2004**, *85* (6), 1066–1068. https://doi.org/10.1063/1.1780597.

(7) Meija, J.; Coplen, T. B.; Berglund, M.; Brand, W. A.; De Bièvre, P.; Gröning, M.; Holden, N. E.; Irrgeher, J.; Loss, R. D.; Walczyk, T.; Prohaska, T. Atomic Weights of the Elements 2013 (IUPAC Technical Report). *Pure and Applied Chemistry*. Walter de Gruyter GmbH March 1, 2016, pp 265–291. https://doi.org/10.1515/pac-2015-0305.

(8) Rahm, M.; Hoffmann, R.; Ashcroft, N. W. Atomic and Ionic Radii of Elements 1-96. *Chemistry – A European Journal* **2016**, *22* (41), 14625–14632. https://doi.org/10.1002/chem.201602949.

(9) Heck, W. B.; Johnson, R. L. Aluminum Alkyls - Safe Handling. *Ind Eng Chem* **1962**, *54* (12), 35–38.

(10) Potts, S. E.; Dingemans, G.; Lachaud, C.; Kessels, W. M. M. Plasma-Enhanced and Thermal Atomic Layer Deposition of Al2O3 Using Dimethylaluminum Isopropoxide, [Al(CH3)2(μ-O i Pr)]2, as an Alternative Aluminum Precursor. *Journal of Vacuum Science & Technology A: Vacuum, Surfaces, and Films* **2012**, *30* (2), 021505-1-021505–021512. https://doi.org/10.1116/1.3683057.

(11) Buttera, S. C.; Mandia, D. J.; Barry, S. T. Tris(Dimethylamido)Aluminum(III): An Overlooked Atomic Layer Deposition Precursor. *Journal of Vacuum Science & Technology A: Vacuum, Surfaces, and Films* **2017**, *35* (1), 01B128-01B128-7. https://doi.org/10.1116/1.4972469.

(12) Katz, A.; Feingold, A.; Pearton, S. J.; Nakahara, S.; Ellington, M.; Chakrabarti, U. K.; Geva, M.; Lane, E. Properties of Titanium Nitride Thin Films Deposited by Rapid-Thermal-Low- Pressure-Metalorganic-Chemical-Vapor-Deposition Technique Using Tetrakis (Dimethylamido) Titanium Precursor. *J Appl Phys* **1991**, *70* (7), 3666–3677. https://doi.org/10.1063/1.349214.

(13) Dean, J. A. *Lange's Handbook of Chemistry*, Fifteenth Edition.; McGRAW-HILL, INC., 1999.

(14) Yartys, V. A.; Denys, R. V.; Maehlen, J. P.; Frommen, C.; Fichtner, M.; Bulychev, B. M.; Emerich, H. Double-Bridge Bonding of Aluminium and Hydrogen in the Crystal Structure of γ-AlH3. *Inorg Chem* **2007**, *46* (4), 1051–1055. https://doi.org/10.1021/ic0617487.

(15) Zapata-Solvas, E.; Hadi, M. A.; Horlait, D.; Parfitt, D. C.; Thibaud, A.; Chroneos, A.; Lee, W. E. Synthesis and Physical Properties of (Zr1−x,Tix)3AlC2 MAX Phases. *Journal of the American Ceramic Society* **2017**, *100* (8), 3393–3401. https://doi.org/10.1111/jace.14870.

(16) Webb, S. P.; Gordon, M. S. *The Dimerization of TiH4*; 1995; Vol. 117. https://pubs.acs.org/sharingguidelines.

(17) Hood, D. M.; Pitzer, R. M.; Schaefer, H. F. Electronic Structure of Homoleptic Transition Metal Hydrides: TiH4, VH4, CrH4, MnH4, FeH4, CoH4, and NiH4. *J Chem Phys* **1979**, *71* (2), 705–712. https://doi.org/10.1063/1.438357.

(18) Magnuson, M.; Mattesini, M.; Li, S.; Höglund, C.; Beckers, M.; Hultman, L.; Eriksson, O. Bonding Mechanism in the Nitrides Ti2AlN and TiN: An Experimental and Theoretical Investigation. *Phys Rev B* **2007**, *76*, 195127.

(19) Dahlqvist, M.; Alling, B.; Abrikosov, I. A.; Rosén, J. Phase Stability of Ti2AlC upon Oxygen Incorporation: A First-Principles Investigation. *Phys Rev B Condens Matter Mater Phys* **2010**, *81* (2). https://doi.org/10.1103/PhysRevB.81.024111.

(20) Young, M. J.; Bedford, N. M.; Yanguas-Gil, A.; Letourneau, S.; Coile, M.; Mandia, D. J.; Aoun, B.; Cavanagh, A. S.; George, S. M.; Elam, J. W. Probing the Atomic-Scale Structure of Amorphous Aluminum Oxide Grown by Atomic Layer Deposition. *ACS Appl Mater Interfaces* **2020**, *12* (20), 22804–22814. https://doi.org/10.1021/acsami.0c01905.

(21) Zhao, H.; Yu, M.; Jiang, Z.; Zhou, L.; Song, X. Interfacial Microstructure and Mechanical Properties of Al/Ti Dissimilar Joints Fabricated via Friction Stir Welding. *J Alloys Compd* **2019**, *789*, 139–149. https://doi.org/10.1016/j.jallcom.2019.03.043.

(22) Allen, F. H.; Kennard, O.; Watson, D. G.; Brammer, L.; Orpen, A. G.; Taylor, R. Tables of Bond Lengths Determined by X-Ray and Neutron Diffraction. Part I. Bond Lengths in Organic Compounds. *Journal of the Chemical Society, Perkin Transactions 2* **1987**, S1–S19.